Analogue Coherent TDMA Receiver with Fast Locking to Free-Running Optical Emitters

Bernhard Schrenk, *Member, IEEE,* and Fotini Karinou, *Member, IEEE*

Abstract—As coherent reception technology continues to move downstream the optical telecommunication infrastructure, the complexity of the involved transceiver technology can quickly introduce a techno-economic roadblock. Under this umbrella, we experimentally demonstrate a conceptually simple, single-polarization and analogue coherent homodyne receiver that builds on no more than an optically locked externally modulated laser. We evaluate this coherent homodyne receiver in the context of analogue radio-over-fiber transmission – a demanding application setting, where a small degradation in signal integrity is leading to large reception penalties. We conduct a continuous-mode characterization of the locking methodology, which enables homodyne detection and hence the transparent translation of electrical signals from the optical to the electrical domain during the coherent reception process. Furthermore, the locking dynamics are being investigated for packet-level reception at a 1 MHz frame rate and two time division multiplexed channels, which are sourced by two optical emitters with free-running laser sources. The radio-over-fiber transmission performance is evaluated for 64-ary quadrature amplitude modulated, orthogonal frequency division multiplexed radio with a short guard interval of 2.7 μs between the packet radio signals. A data rate of 0.5 Gb/s over 100 MHz radio bandwidth is obtained at an optical loss budget of >35 dB between transmitter and receiver, without resorting to digital signal processing resources for the purpose of signal recovery. Moreover, a small ~0.3% penalty in error vector magnitude between continuous- and packet-mode confirms the compatibility of the analogue coherent receiver in networks with fast locking requirements.

Index Terms—Optical communication terminals, Optical fiber communication, Optical signal detection, Time division multiplexing, Externally modulated laser, Homodyne detection

I. INTRODUCTION

INCREASED optical loss budgets due to dense and yet passive distribution networks, spectral exhaustion due to a low spectral occupancy that is limited by widely spaced optical filters and simple modulation formats that impose a hard limit for the transmission capacity – all these attract attention in coherent communication technology for the short-reach and access network segments [1, 2]. Although coherent
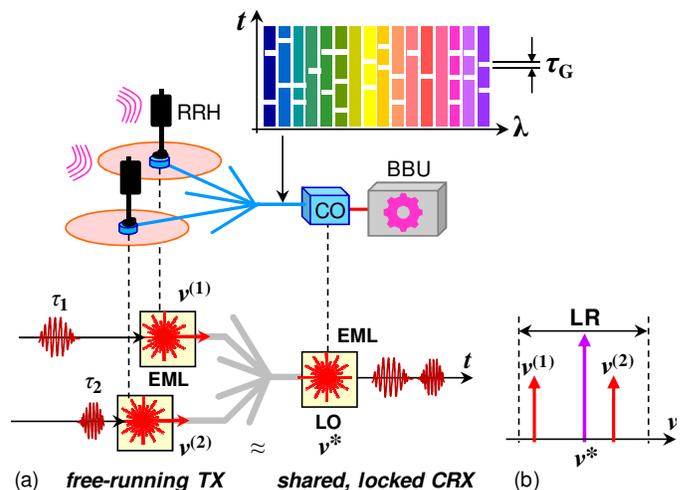
Fig. 1. (a) Coherent homodyne receiver that is locked and time-shared by multiple free-running transmitters. (b) Spectral allocation of free-running transmitter emission frequencies $v^{(1)}, v^{(2)}$ within the injection-locking range LR of the LO v^* of the coherent receiver.

reception is a well-researched topic that has found commercial take-up in metro and core networks since long, the cost associated to these coherent transceivers does not trade favorably against their performance offerings. The specific techno-economic setting in shorter reach networks calls for a coherent approach that is bound to a much lower technological complexity and cost. This puts analogue coherent receivers into the spotlight. Their main motivation is to either substitute digital signal processing (DSP) functions with analogue counterparts, or to apply a disruptive methodology to perform coherent reception. Among these flavors, earlier research works have demonstrated the co-transmission of the optical carrier over a second fiber for homodyne detection of quadrature modulation [3], non-linear analogue processing in combination with intensity modulation [4, 5], half-rate coding to introduce redundancy in a manner that eliminates the need for optical hardware used for polarization control [6], and a simple, laser-based coherent homodyne receiver [7] that also allows for full-duplex transmission [8]. However, the traffic patterns in shorter-reach networks are seldom predictable and in general highly dynamic. Representative examples are the traffic generated in datacenters [9] and in radio access networks [10]. The characteristics of these time-constrained patterns, which can be summarized as short-lived flows and packet-oriented data, require the coherent detection
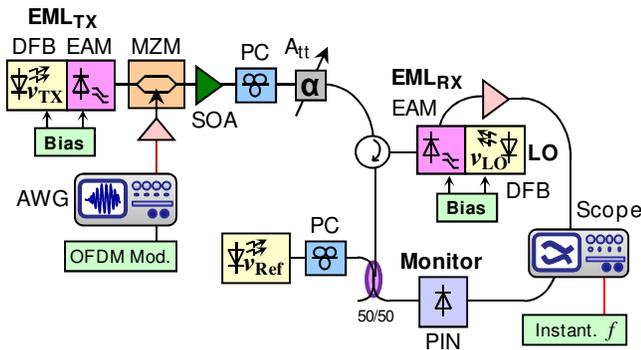
Fig. 2. Experimental setup to characterize locking under continuous-mode.

technology to adapt nanosecond-scale locking for its receiver and, in particular, its local oscillator (LO).

This work aims at analogue coherent reception of packet data originating from two independent optical transmitters. We experimentally investigate that a conceptually simple coherent homodyne receiver based on an externally modulated laser (EML) can swiftly lock on short-lived data packets. Based on our earlier results [11] on analogue radio-over-fiber (RoF) transmission, we show that coherent reception in a time division multiplexed access (TDMA) mode is feasible for orthogonal frequency division multiplexed (OFDM) radio signals with a data payload of 26.3 kByte. We will prove that no digital resources are required in virtue of the all-optical scheme that is applied to ensure locking of the coherent receiver, even though two free-running optical sources are used at the data transmitters. As such, a fully analogue and radio frequency (RF) transparent coherent optical link is provided.

This paper is organized as follows. Section II introduces the coherent homodyne receiver architecture with all-optical LO locking. Section III investigates the characteristics of the locking process under continuous-mode injection, while Section IV evaluates the locking of the receiver under the injection of packet signals. The transmission performance for analogue RoF signals is presented in Section V. Finally, Section VI concludes the work.

II. All-Optical Locking of an EML-Enabled Coherent Receiver

In the context of this work, coherent detection is employed by a time-shared receiver at the central office (CO). Figure 1(a) illustrates an analogue RoF fronthaul that connects multiple remote radio heads (RRH) to the CO at which the baseband unit (BBU) for radio signal processing is hosted [12]. In such an analogue RoF scenario, a digitization of the radio signal is omitted in virtue of high-fidelity opto-electronic conversions at transmitter [13] and receiver so that the radio signal is transparently conveyed over the optical fiber infrastructure [14]. In order to increase the flexibility at this potentially dense fronthaul network, wavelengths are time-shared among multiple transmitters following a suitable medium-transparent medium access control protocol that spans over both, radio and optical domains [15]. In this way,

the traffic dynamics as they apply to wireless access [10] can be flexibly addressed at the optical layer, provided that dynamic opto-electronic transceiver sub-systems are employed.

This implies the coherent reception (CRX) of signals that originate from multiple data transmitters and essentially requires the synchronization of the LO ($v*$) with all source lasers $v^{(i)}$ under packet operation, ideally without employing an extra training signal. The particular emission frequencies, denoted as $v^{(1)}, v^{(2)}$ in Fig. 1(b), will differ but will be in the spectral vicinity of $v*$. To master the synchronization, a digital CRX will adopt fast frequency offset and carrier phase recovery [16] that are sequentially applied to the incident optical packets spaced by a short guard interval τ_G. In order to overcome the costly digital signal processing (DSP) resources for this process, which would strongly contradict the low-complexity flavor of the analogue RoF transmission in a cloud-based setting [12], an analogue CRX methodology is of utmost importance.

One possible way to achieve the required synchronization of the CRX to all transmitters, while avoiding extra DSP functions, is to exploit all-optical locking of the LO. The off-loading of this essential key function to the optical domain retains the possibility to provide a truly lean analogue CRX solution as earlier demonstrated for continuous-mode RoF signals [17]: As a matter of fact, the analogue CRX that is investigated in this work builds on nothing more than an EML. A precise frequency translation from the optical to the electrical domain is achieved through an all-optical locking scheme. For this purpose, the distributed feedback (DFB) section of the EML is injection-locked to a portion of the incident RoF signal at $v^{(i)}$. This process requires that the detuning $|v^{(i)} – v*|$ of the optical frequencies for the RoF signal and the LO is smaller than the locking range LR [18]. Figure 1(b) shows this condition for two independent RoF signals within the LR of the CRX, which is typically in the range of 0.1 to 1 GHz for commonly used optical injection levels [8]. Coarse and fine tuning of either the transmitted optical frequency or the LO can be facilitated by either temperature or bias current control of the EML [19, 20]. Operation in wavelength-multiplexed transmission schemes would require a wider tuning range or an alternative tuning mechanism for the laser.

After synchronizing the LO to the data at the optical input port of the EML, the RoF signal is correctly detected through the electro-absorption modulator (EAM). Under reverse bias the EAM provides the function of a fast photodiode, which completes the requirements of a single-polarization homodyne CRX. Polarization immunity would require a second EML branch in a polarization diversity arrangement, as demonstrated earlier [21]. In this way, active polarization tracking can be avoided at the expense of a second receiver branch. This implementation detail was omitted in the present work for the sake of simplicity. Instead, the investigation focuses on the performance of this CRX under TDMA operation. This includes the analysis of locking dynamics under optical input signals in continuous- and packet-mode and a performance assessment for coherent analogue RoF reception in TDMA with two free-running RoF transmitters having a small guard interval of a few microseconds.
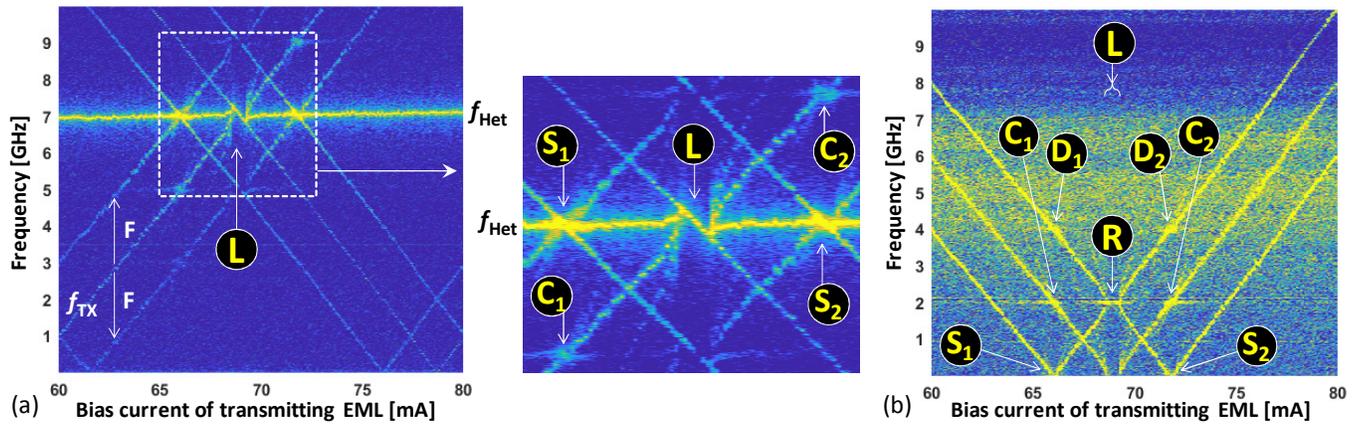
Fig. 3. Signal spectrum acquired at (a) the monitor receiver after heterodyning with a reference laser and (b) at the EML$_{RX}$. The color scale that indicates the intensity is logarithmic.
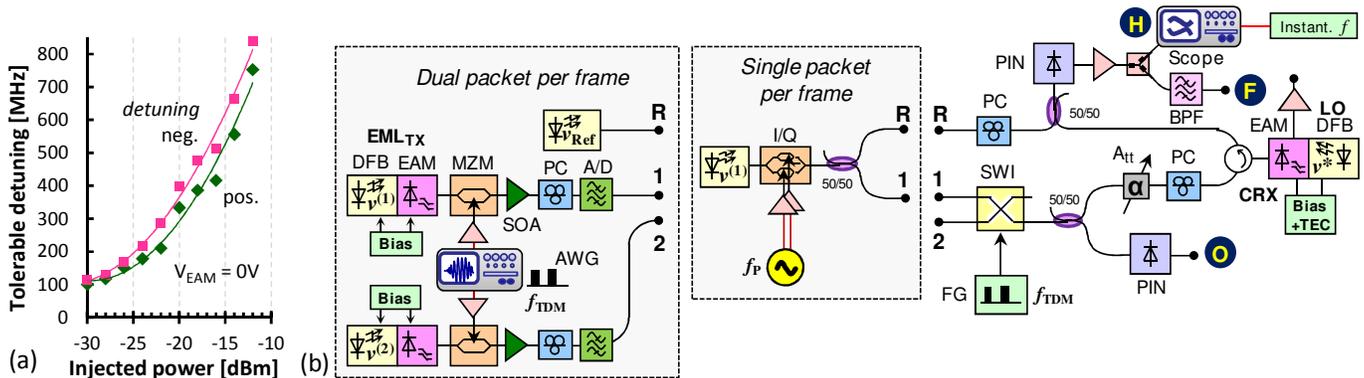
Fig. 4. (a) Range of injection locking for the EML. (b) Experimental setup to characterize the locking process of the coherent receiver under packet injection.

III. LOCKING CHARACTERISTICS UNDER CONTINUOUS-MODE OPERATION

First, the locking characteristics are experimentally studied for continuous-mode radio signal transmission. Figure 2 presents the characterization setup. A RoF transmitter based on an EML and a Mach-Zehnder modulator (MZM) modulate the optical carrier frequency v_{TX} with an orthogonal frequency division multiplexed (OFDM) radio signal. The OFDM carrier frequency F was 2 GHz and the radio signal bandwidth was 125 MHz. The signal is amplified by a semiconductor optical amplifier (SOA) and injected at a power level of -25 dBm into the coherent EML-based receiver. The same EML devices were used at transmitter and receiver. In order to acquire the instantaneous optical frequency for the LO of the coherent receiver, its output, which is composed by the LO (v_{LO}) and further by a small portion of the received signal due to the reflectance of the EML$_{RX}$, is beating against a reference laser (v_{Ref}) at an optical monitor. This reference is detuned from the free-running EML$_{RX}$ wavelength for the purpose of heterodyning and the beating signal is acquired through a real-time oscilloscope for further signal analysis. The spectral characteristics over a range much wider than the locking range of the EML$_{RX}$ can be observed through a swept optical transmitter frequency v_{TX}. This is realized through a continuous adjustment of the DFB bias current of the corresponding EML$_{TX}$. The received electrical signal at the EML$_{RX}$ is acquired additionally to yield the signal characteristics for coherent homodyne detection.

Figure 3(a) presents the electrical beating spectrum at the monitor for a detuning of the bias current at EML$_{TX}$. This detuning leads to a wavelength shift in the received RoF signal and an eventual lock of the receiving EML$_{RX}$.

The beat note between EML$_{RX}$ at v_{LO} and the reference laser at v_{Ref} is clearly visible at ~7 GHz. The detected RoF signal at f_{TX} shows the double-sideband radio signal that is spaced by F = 2 GHz from the optical carrier. It evolves over the acquired frequency range as the EML$_{TX}$ bias current at the transmitter is increased, together with a mirror frequency in reference to the heterodyne frequency $f_{Het} = |v_{Ref} - v_{LO}|$. The spectral evolution follows a tuning efficiency of 0.67 GHz/mA. When the beat note of the optical carrier of the RoF signal reaches the heterodyne frequency between the free-running EML$_{RX}$ and the reference laser, meaning that the wavelengths of EML$_{RX}$ and EML$_{TX}$ match, the heterodyne frequency follows the evolution of the RoF signal (L). This is explained by the injection locking that applies when the two EML wavelengths are spectrally allocated within the locking range. Figure 4(a) shows this frequency range, in which a detuning between the lasers is small enough to accomplish locking for the LO. The locking range, defined as the sum of positive (◆) and negative (■) detuning $v_{TX} - v_{LO}$, is 500 MHz for an injected power of -22 dBm. A low emission wavelength drift leads to stable long-term locking, similarly as reported earlier [8]. Under this locking condition, EML$_{RX}$ does not show a free-running behavior anymore, which interrupts the spectral line of the
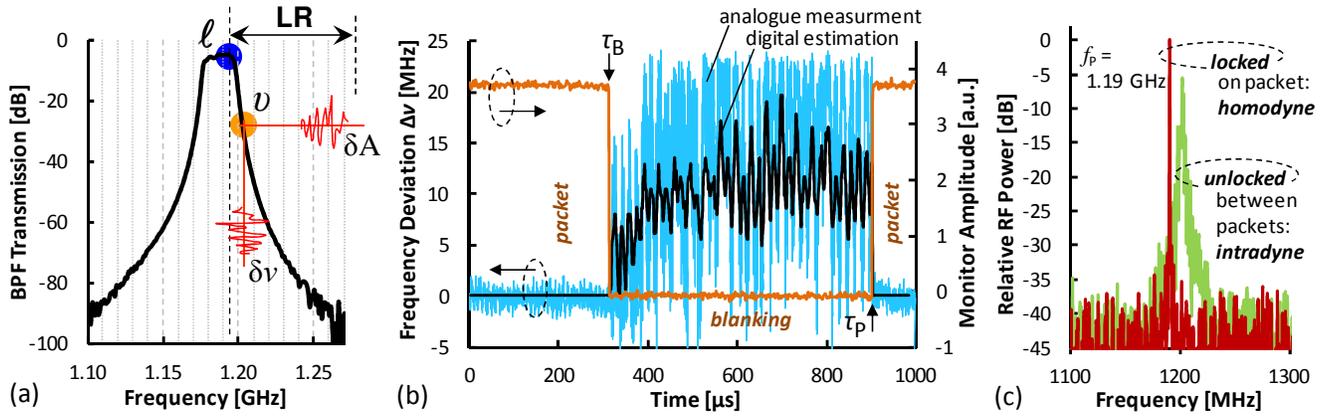
Fig. 5. (a) Transmission of the RF bandpass filter applied for frequency discrimination. (b) Frequency deviation of the pilot tone. (c) Pilot tone spectrum in presence and absence of an injected packet.
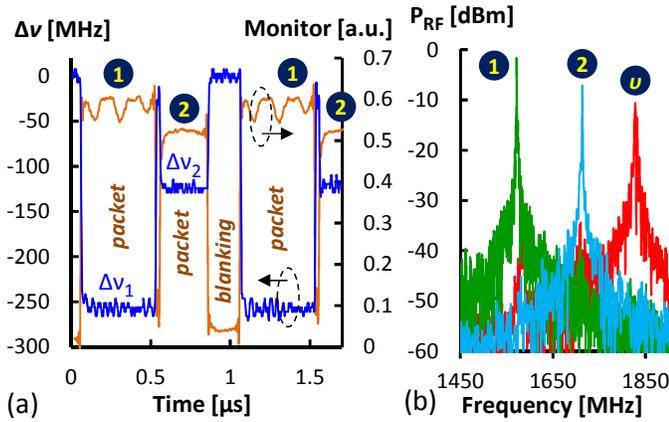
Fig. 6. Locking characteristics for dual-packet injection. (a) Frequency deviation and (b) beating spectra.

heterodyne frequency between 68.6 and 69.3 mA of the transmitter-side bias current. While it is intended to facilitate locking through the optical carrier, the sub-carriers of the OFDM signal similarly induce locking. This is visible at points S_1 and S_2, for which the optical carrier appears at 2 GHz (C_1,C_2) relative to the heterodyne frequency.

The signal spectrum that is received by EML_{RX} is presented in Fig. 3(b). The optical carrier of the RoF signal moves towards that of the EML_{RX} (f = 0 Hz). Within the locking range (L), the beat note between the two optical carriers disappears and the RoF signal is visible at the OFDM carrier frequency of 2 GHz (R). For a further increase of the EML_{TX} bias current the EML_{RX} gets unlocked and the RoF signal evolves steadily towards higher beat note frequencies. It can be noticed that the OFDM signal leads to sporadic locking of the EML_{RX} when one of the sidebands coincide with its optical carrier (S_1, S_2). In these cases the optical carrier shows a beat note at 2 GHz (C_1,C_2), while the other sideband appears at 4 GHz (D_1,D_2). The locking range (at f = 0 Hz) is only weakly pronounced due to the low power in the constituent sub-carriers of the OFDM signal.

IV.   RECEIVER LOCKING AT THE PACKET LEVEL

A. Locking through packet injection

In order to conduct coherent homodyne detection, it is

paramount for the coherent receiver to swiftly lock on the incident data packet. This essential property was characterized for the EML-based CRX using the setup shown in Fig. 4(b). As for the characterization, identical EML devices are used as optical sources at the transmitters and as the receiver. At the optical transmitter, a pilot tone at f_P = 1.19 GHz is single-sideband modulated on the optical carrier $v^{(1)}$ for later analysis of the pilot tone integrity after coherent reception. This data signal at $v^{(1)}$ is sliced into packets through an optical switch (SWI) that is operated at a repetition rate in the millisecond range and at a duty cycle of 50%. The generated optical packet with blanked optical intensity before and after the packet is monitored (O) and further injected to the CRX after manual polarization control (PC). The injection level was -25 dBm. In order to enable locking, the wavelength of the injected signal is tuned to 1548.05 nm. With this it falls within the wavelength channel of the CRX, which was operated at 40°C. Coarse temperature and fine current tuning place the signal within the locking range. In a realistic deployment a signaling channel would have to be implemented in order to find and lock to the correct transmission channel, similar as it is implemented in optical access systems. However, the EML-based CRX can assist this task by serving as tunable spectrum analyzer with high resolution [22].

In order to analyze the instantaneous locking response, the beating of the CRX output at v^* and the uncarved data signal at $v^{(1)}$ is acquired through a photodetector (H). The effect of packet reception on the CRX locking can be determined by investigating the instantaneous frequency of the pilot tone. Instead of relying on a purely digital frequency estimation for this task, an analogue RF bandpass filter (BPF) has been additionally employed as frequency discriminator (F) after the photodetector. The spectrally narrow BPF transmission is presented in Fig. 5(a). It translates unlocked operation (υ) associated to the blanking of the optical input signal to the CRX into amplitude fluctuations δA that arise from the optical emission frequency drift δv of the free-running LO. For the locked case, a steady output is obtained instead.

Figure 5(b) presents the packet trace obtained through the monitor photodetector and the measured frequency deviation Δv, which is plotted as difference between the actual beat note
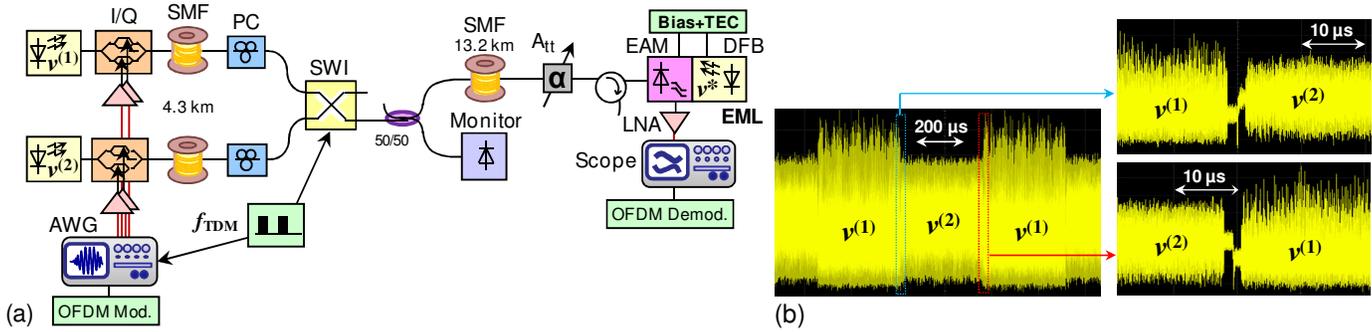
Fig. 7. (a) Transmission setup for evaluating the analogue RoF performance. (b) TDMA frame and transitions between the TDMA channels.
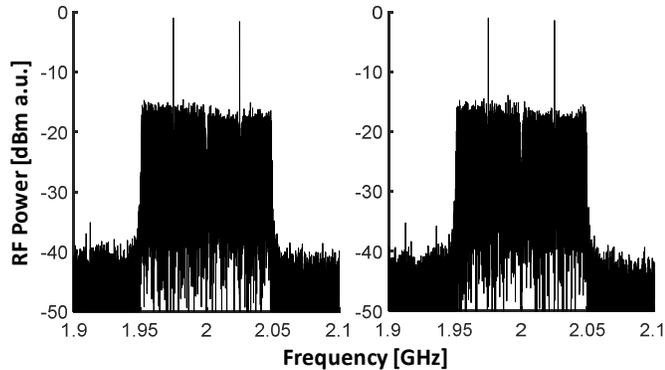
Fig. 8. Received RoF spectra at both TDMA channels.

frequency and the set pilot frequency f_P. This deviation is reported for both, analogue and digital instantaneous frequency measurement.

When the packet is present, meaning optical injection to the EML-based CRX, the actual and set frequencies match so that $\Delta v = 0$. This is an indication for stable locking, leading to coherent homodyne reception with $v^* = v^{(1)}$. At the packet edge, once the optical intensity blanks (τ_B), the lock of the LO is lost and the homodyne reception would turn into an intradyne with $v^* \approx v^{(1)}$, meaning that the LO of the CRX is free-running. This difference can be also noticed in the beat note spectra at point H for a present and absent data packet. Figure 5(c) shows a clear pilot frequency f_P for the homodyne (locked) detection, in contrary to the smeared-out pilot during intradyne (unlocked) reception.

The received beat note shows a deviation of $\Delta v < 25$ MHz after instantaneous frequency estimation in the digital domain (H) and also through direct analogue acquisition using the BPF slope (F). This value aligns with the typical drift of temperature-stabilized DFB lasers. Moreover, it is less than the locking range of >100 MHz, which is paramount to obtain locking at the next rising packet edge: The LO of the CRX locks again at the begin of the next packet (τ_P), leading to the desired homodyne condition: $\Delta v = 0$. The locking and unlocking processes appear to be fast and without noticeable lag. This means that a very short pre- and postamble is sufficient at the package edges, which is acceptable for short-lived data flows and packet-centric data. These results indicate correct analogue CRX operation for single packet reception.

B. Fast dual-channel TDMA frame

In addition, the locking characteristics have been evaluated for a TDMA frame with two packets. For this reason, the setup of Fig. 4(b) has been slightly modified. First, the switch ports (1,2) are fed by two optical packet envelope emitters at $v^{(1)}$ and $v^{(2)}$. These emitters include an EML as source laser, a MZM as packet carver and a SOA as booster amplifier with subsequent 100 GHz add-drop (A/D) filter to suppress optical broadband noise. In this way, without exclusively resorting to the electrically synchronized optical switch for the purpose of slot generation, a short blanking occurs between the two TDMA channels. Moreover, the TDMA timing was changed to a faster 1 MHz frame rate and the duty cycles for the two TDMA channels were 47% and 30%, which also leaves a blanked slot within the TDMA frame. Second, a stable laser (v_{Ref}) supplies the optical reference port (R) of the heterodyning receiver. In this way the frequency deviation due to both packets can be analyzed with respect to the blanked packet, for which the LO of the CRX becomes a free-running rather than a locked optical source.

Figure 6(a) shows the obtained frequency deviation Δv after digital instant frequency analysis in relation to the optically monitored packet envelopes. Figure 6(b) reports the optical spectrum received at the heterodyne receiver (point H in Fig. 4(b)), which comprises the beating frequencies for the two TDMA channels (1,2) and the unlocked LO at the CRX (υ). The difference in beating frequencies agree with the instantaneous frequency obtained through digital estimation. These two deviations in Fig. 6(a), which are following the packet envelope of the injected TDMA signal to the CRX, are $\Delta v_1 = -256$ MHz and $\Delta v_2 = -114$ MHz.

Moreover, the locking speed is well below 100 ns, which is supported by earlier theoretical studies [23]. This value suits radio-over-fiber communication that delivers wireless signals with much larger frame overheads in the µs range [24].

V. COHERENT HOMODYNE ANALOGUE RADIO-OVER-FIBER TRANSMISSION UNDER TDMA OPERATION

A. Experimental setup

The data-centric RoF transmission performance was evaluated using the setup shown in Fig. 7(a). Two narrowband OFDM signals with 64 sub-carriers over a bandwidth of 100 MHz were modulated on a RF carrier frequency of 2 GHz and
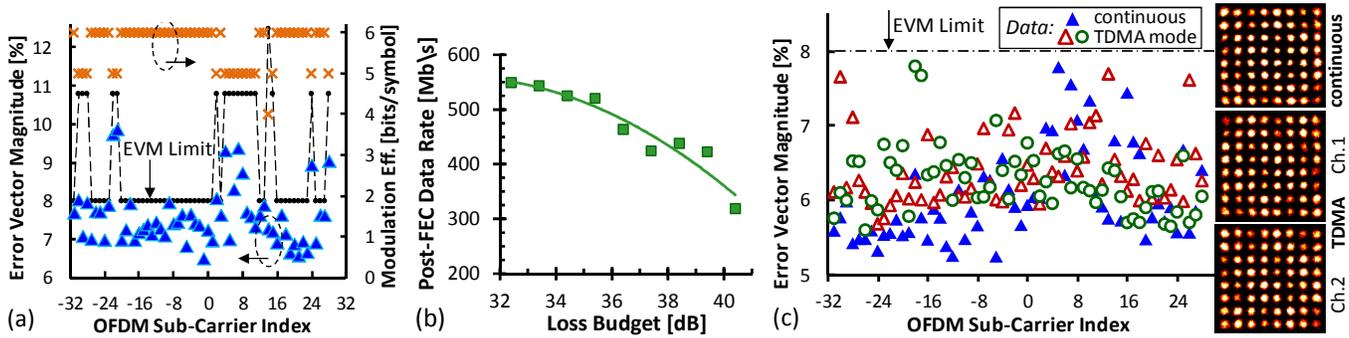
Fig. 9.   (a) Continuous-mode OFDM performance for an optical loss budget of 35.4 dB and (b) supported data rate as function of the loss budget. (c) Comparison between the performance in continuous- and TDMA-mode at a loss budget of 32.4 dB. All sub-carriers were loaded with 64-QAM.

launched with 3 dBm. Two packets of 350 μs length each were allocated in a TDMA frame. The guard interval at the begin and end of each packet was 1.35 μs. Depending on the bit loading, each packet carries about 17.5 to 26.3 kByte of data for 16-QAM to 64-QAM, respectively.

The TDMA frame is optically generated through use of an optical switch. The two optical OFDM emitters at $\nu^{(1)}$ and $\nu^{(2)}$ feed the switch inputs and are time-sharing its output. The switch also acts as optical gate that blanks the continuous-wave emission at the transmitters when data modulation is absent. Figure 7(b) shows the monitored TDMA signal and the transition between two TDMA channels.

The RoF signals are transmitted over drop spans with 4.3 km of standard single-mode fiber (SMF) and a feeder fiber of 13.2 km. The optical loss budget between transmitter branches and CRX was set with a variable optical attenuator (A_{tt}).

The TDMA signal is eventually received by the EML-based CRX. A 50Ω low-noise amplifier (LNA) is used as RF front-end. The OFDM signal was demodulated through off-line DSP. No further digital signal processing resources were applied despite coherent reception of the TDMA frame.

B. Results and discussion

The RF spectrum of the received signal, which is reported in Fig. 8, confirms the integrity of the RoF signal despite analogue coherent homodyne detection. The OFDM boundaries are clearly delimited and its two pilot tones can be recognized as sharp rather than smeared out spectral lines.

Continuous-mode RoF transmission using a single optical transmitter with a continuous RoF signal at $\nu^{(1)}$ was first evaluated as a performance reference. In this case all OFDM sub-carriers can be loaded with 64-ary quadrature amplitude modulation (QAM) for an optical loss budget of 32.4 dB. The average error vector magnitude (EVM) was 6.04% and therefore well below the 64-QAM EVM limit of 8%. A bit error ratio (BER) of $2.17{\times}10^{-3}$ has been estimated for this EVM value after error counting. Figure 9(a) presents the EVM (▲) and the bit loading (×) over the OFDM sub-carrier index for a loss budget of 35.4 dB, at which an average modulation efficiency of 5.7 bits/symbol can still be obtained. Considering a hard-decision forward error correction (FEC) with a typical FEC overhead of 7%, a post-FEC data rate of 0.52 Gb/s can be achieved for this narrowband OFDM signal.

The dependence of the supported data rate (■) and the

modulation efficiency (●) on the optical loss budget is reported in Fig. 9(b). A modulation efficiency of 4 bits/symbol is supported at a high loss budget of 39.8 dB, even though a sub-optical LNA front-end is applied after the EML-based CRX. This validates the correct operation of the analogue homodyne receiver even under low delivered optical power.

The transmission performance for dual-channel TDMA operation at $\nu^{(1)}$ and $\nu^{(2)}$ is presented in Fig. 9(c). The average EVM obtained for both TDMA channels does not show a strong degradation. Compared to the 6.04% in continuous-mode operation (▲) as mentioned earlier, the EVM for the two TDMA channels is 6.4% (△) and 6.26% (○) and therefore marginally higher. The corresponding BER values are $2.59{\times}10^{-3}$ and $2.41{\times}10^{-3}$. The average margin to the 64-QAM EVM limit remains as high as 1.7% in the worst case. Figure 9(c) also compares the 64-QAM constellation diagrams for continuous- and TDMA-mode. These RoF transmission results evidence that the low-complexity EML-based coherent receiver is correctly locking under packet operation with a small guard time of $\tau_G = 2.7$ μs.

VI. CONCLUSION

A conceptually simple single-polarization coherent receiver based on an EML has been demonstrated for RoF transmission in continuous and TDMA operation mode. Homodyne reception is obtained through all-optical and thus fast locking of the LO, re-using the incident data signals as injection seed. The characteristics in terms of locking range and dynamics have been investigated in both modes of operation. Instantaneous optical synchronization of the LO emission frequency has been validated for packet-centric reception at 1 MHz TDMA frame rate and with two TDMA channels, which have been sourced by independent, free-running lasers.

RoF transmission with a short TDMA guard interval of 2.7 μs has been experimentally studied. A post-FEC data rate of 0.5 Gb/s over 100 MHz OFDM bandwidth was obtained at an optical budget of >35 dB. A small ~0.3% EVM penalty between TDMA- and continuous-mode reception was noticed, which renders the proposed coherent receiver as compatible with TDMA operation.

The applied homodyne reception methodology enables a fully analogue coherent detection scheme that does not require additional DSP functions to recover the signal integrity for the

radio signal, such as it would be required for coherent intradyne detection. Further improvement in terms of reception sensitivity and wideband operation is expected when replacing the current 50Ω LNA after the EML-based detector with a transimpedance amplifier.

REFERENCES

[1] E. Ip, A. Lau, D. Barros, and J. Kahn, "Coherent detection in optical fiber systems," *OSA Opt. Expr.*, vol. 16, no. 2, pp. 753-791, Jan. 2008.

[2] M. Sezer Erkilinc *et al.*, "Comparison of Low Complexity Coherent Receivers for UDWDM-PONs (λ-to-the-User)," *IEEE/OSA J. Lightwave Technol.*, vol. 36, no. 16, pp. 3453-3464, Aug. 2018.

[3] M. Morsy-Osman *et al.*, "DSP-free 'coherent-lite' transceiver for next generation single wavelength optical intradatacenter interconnects," *OSA Opt. Expr.*, vol. 26, no. 7, pp. 8890-8903, Apr. 2018.

[4] M. Artiglia, M. Presi, F. Bottoni, M. Rannello, and E. Ciaramella, "Polarization-Independent Coherent Real-Time Analog Receiver for PON Access Systems," *IEEE/OSA J. Lightwave Technol.*, vol. 34, no. 8, pp. 2027-2033, Apr. 2016.

[5] J. Altabas *et al.*, "Real-Time 10 Gbps Polarization Independent Quasicoherent Receiver for NG-PON2 Access Networks," *IEEE/OSA J. Lightwave Technol.*, vol. 37, no. 2, pp. 651-656, Jan. 2019.

[6] M.S. Faruk, D.J. Ives, and S.J. Savory, "Technology Requirements for an Alamouti-Coded 100 Gb/s Digital Coherent Receiver Using 3×3 Couplers for Passive Optical Networks," *IEEE Phot. J.*, vol. 10, no. 1, p. 7200313, Feb. 2018.

[7] B. Schrenk, "Injection-Locked Coherent Reception Through Externally Modulated Laser," *IEEE J. Sel. Topics in Quantum Electron.*, vol. 24, no. 2, p. 3900207, Mar. 2018.

[8] B. Schrenk, and F. Karinou, "A Coherent Homodyne TO-Can Transceiver as Simple as an EML," *IEEE/OSA J. Lightwave Technol.*, vol. 37, no. 2, pp. 555-561, Jan. 2019.

[9] T. Benson, A. Akella, and D.A. Maltz, "Network Traffic Characteristics of Data Centers in the Wild," in *Proc. ACM SIGCOMM Conf. Internet Meas.*, Melbourne, Australia, Nov. 2010, p. 267.

[10] U. Paul, A. Subramanian, M. Buddhikot, and S. Das, "Understanding traffic dynamics in cellular data networks," in *Proc. INFOCOM*, Shanghai, China, Apr. 2011, pp. 882–890.

[11] B. Schrenk, and F. Karinou, "Low-Cost Analogue Coherent TDMA Receiver with All-Optical Synchronization to Free-Running Optical Carriers," in *Proc. Opt. Fiber Comm. Conf.*, San Diego, USA, Mar. 2019, M4F.6

[12] C. Pan, M. Elkashlan, J. Wang, J. Yuan, and L. Hanzo, "User-Centric C-RAN Architecture for Ultra-Dense 5G Networks: Challenges and Methodologies," *IEEE Comm. Mag.*, vol. 56, no. 6, pp. 14-20, Dec. 2017.

[13] B.G. Kim, S.H. Bae, H. Kim, and Yun C. Chung, "RoF-Based Mobile Fronthaul Networks Implemented by Using DML and EML for 5G Wireless Communication Systems," *IEEE/OSA J. Lightwave Technol.*, vol. 36, no. 14, pp. 2874-2881, Jul. 2018.

[14] P. T. Dat, A. Kanno, N. Yamamoto, and T. Kawanishi, "Seamless Convergence of Fiber and Wireless Systems for 5G and Beyond Networks," *IEEE/OSA J. Lightwave Technol.*, vol. 37, no. 2, pp. 592-605, Jan. 2019.

[15] G. Kalfas, and N. Pleros, "An Agile and Medium-Transparent MAC Protocol for 60 GHz Radio-Over-Fiber Local Access Networks," *IEEE/OSA J. Lightwave Technol.*, vol. 28, no. 16, pp. 2315-2326, Aug. 2010.

[16] F. Vacondio *et al.*, "Flexible TDMA Access Optical Networks Enabled by Burst-mode Software Defined Coherent Transponders," in *Proc. Europ. Conf. Opt. Comm.*, London, United Kingdom, Sep. 2013, We.1.F.2.

[17] B. Schrenk, "The EML as Analogue Radio-over-Fiber Transceiver – a Coherent Homodyne Approach," *IEEE/OSA J. Lightwave Technol.*, vol. 37, no. 12, pp. 2866-2872, Jun. 2019.

[18] F. Mogensen, H. Olesen, and G. Jacobsen, "Locking Conditions and Stability Properties for a Semiconductor Laser with External Light Injection," *IEEE J. Quantum Electron.*, vol. 21, no. 7, pp. 784-793, Jul. 1985.

[19] J.A. McCaulley, M. Donnelly, M. Vernon, and I. Taha, "Temperature dependence of the near-infrared refractive index of silicon, gallium arsenide, and indium phosphide," *APS Phys. Rev. B*, vol. 49, no. 11, p. 7408, Mar. 1994.

[20] B.R. Bennett, R.A. Soref, and J.A. Del Alamo, "Carrier-Induced Change in Refractive Index of Inp, GaAs, and InGaAsP," *IEEE J. Quantum Electron.*, vol. 26, no. 1, pp. 113-122, Jan. 1990.

[21] B. Schrenk, and F. Karinou, "Simple Laser Transmitter Pair as Polarization-Independent Coherent Homodyne Detector," *OSA Opt. Expr.*, vol. 27, no. 10, pp. 13942-13950, May 2019.

[22] B. Schrenk, and F. Karinou, "EML Transmitter as Coherent Monitor for Distributed Spectrum Snooping", in *Proc. Europ. Conf. Opt. Comm.*, Dublin, Ireland, Sep. 2019, P18.

[23] P. Spano, M. Tamburrini, and S. Piazzolla, "Optical FSK Modulation Using Injection-Locked Laser Diodes," *IEEE/OSA J. Lightwave Technol.*, vol. 7, no. 4, pp. 726-728, Apr. 1989.

[24] S.Y. Lien, S.L. Shieh, Y. Huang, B. Su, Y.L. Hsu, and H.Y. Wei, "5G New Radio: Waveform, Frame Structure, Multiple Access, and Initial Access," *IEEE Comm. Mag.*, vol. 55, no. 6, pp. 64-71, Jun. 2017.

Bernhard Schrenk (S'10-M'11) was born 1982 in Austria and received the M.Sc. ('07) degree in microelectronics from the Technical University of Vienna. He was at the Institute of Experimental Physics of Prof. A. Zeilinger, where he was involved in the realization of a first commercial prototype for a quantum cryptography system, within the European SECOQC project. From 2007 to early 2011 he obtained his Ph.D degree at UPC BarcelonaTech, Spain. His Ph.D thesis on multi-functional optical network units for next-generation Fiber-to-the-Home access networks was carried out within the FP7 SARDANA and EURO-FOS projects. In 2011 he joined the Photonic Communications Research Laboratory at NTUA, Athens, as post-doctoral researcher and established his research activities on coherent FTTH under the umbrella of the FP7 GALACTICO project. In 2013 he established his own research force on photonic communications at AIT Austrian Institute of Technology, Vienna, where he is working towards next-generation metro-access-5G networks, photonics integration technologies and quantum optics.

Dr. Schrenk has authored and co-authored ~140 publications in top-of-the-line (IEEE, OSA) journals and presentations in the most prestigious and highly competitive optical fiber technology conferences. He was further awarded with the Photonics21 Student Innovation Award and the Euro-Fos Student Research Award for his PhD thesis, honoring not only his R&D work but also its relevance for the photonics industry. He was elected as Board-of-Stakeholder member of the Photonics21 European Technology Platform in 2017. During his extensive research activities he was and is still engaged in several European projects such as SARDANA, BONE, BOOM, APACHE, GALACTICO, EURO-FOS and the Quantum Flagship project UNIQORN. In 2013 he received the European Marie-Curie Integration Grant WARP-5. In 2018 he was awarded by the European Research Council with the ERC Starting Grant COYOTE, which envisions coherent optics everywhere.

Fotini Karinou (S'09-M'13) was born in Arta, Greece, in 1983. She received the Diploma in Electrical and Computer Engineering, with specialization in telecommunications and information theory, and the PhD degree in optical communications focused on spectrally efficient WDM optical interconnect networks with advanced modulation formats, from the University of Patras, Greece, in 2007, and 2012, respectively. In 2007, she was a visiting researcher in the Institute for Quantum Optics and Quantum Information (IQOQI), at Vienna University of Technology, participating in the initial attempts for the realization of a commercial prototype of a quantum key distribution (QKD) system based on polarization entanglement in the Institute of Experimental Physics of Prof. Zeilinger. In 2011 to 2012, she was a visiting researcher at Denmark Technical University, Photonics Department, where she worked toward spectrum-flexible cognitive optical networks, hybrid optical fiber-wireless transmission and advanced modulation techniques for high-performance computing optical interconnects. From February 2013 to June 2018, Dr. Karinou worked as a Senior R&D Engineer in the Optical Technology Department, later restructured to Optical & Quantum Laboratory, at Huawei Technologies Duesseldorf GmbH, in the German Research Center in Munich, toward next generation high-capacity coherent systems for long reach, high data-rate metro/access optical networks, optical interconnects for data centers and quantum communications. In July 2018 she joined the Systems and Networking Group at Microsoft Research Ltd in Cambridge, UK, where she is working toward developing optical technologies for next generation cloud computing systems and networks. She has authored and co-authored 70 publications in the highest prestigious optical communications technology journals and conferences. Dr. Karinou has been engaged in several European research projects such as EU FP6 SECOQC, EU FP7 ICT-BONE, EU FP7 CHRON, and H2020 ROAM projects.